Journal of Hazardous Materials 192 (2011) 168–175

Contents lists available at ScienceDirect

Journal of Hazardous Materials

journal homepage: www.elsevier.com/locate/jhazmat

Enhanced sorption of radiocobalt from water by Bi(III) modified montmorillonite: A novel adsorbent

Zhiqiang Guo[a], Yuan Li[b], Shouwei Zhang[a], Haihong Niu[a], Zhesheng Chen[a], Jinzhang Xu[a,*]

[a] School of Nuclear Science and Technology, Lanzhou University, 730000, Lanzhou, PR China
[b] State Key Laboratory of Quantum Optics and Quantum Optics Devices, Institute of Opto-Electronics, Shanxi University, 030006, Taiyuan, PR China

ARTICLE INFO

Article history:
Received 10 January 2011
Received in revised form 12 April 2011
Accepted 1 May 2011
Available online 10 May 2011

Keywords:
Co(II)
Sorption
Bi–montmorillonite
Kinetics
Thermodynamic parameter

ABSTRACT

In this study, Ca–montmorillonite (Ca–Mt) modified with Bi^{3+} was used as a novel adsorbent for the sorption of Co(II) from aqueous solutions. The sorption of Co(II) on Bi–montmorillonite (Bi–Mt) was investigated as a function of contact time, pH, ionic strength, adsorbent content, Co(II) concentrations, fulvic acid (FA) and temperature. Compared to Ca–Mt, Bi–Mt showed a higher affinity to bind Co(II) ions. The sorption percentage of Co(II) on Bi–Mt increased with increasing pH at pH 3.0–8.5, and then maintained the high level at pH 8.5–12. The sorption of Co(II) on Bi–Mt was dependent on ionic strength at low pH, and independent of ionic strength at high pH. The presence of FA enhanced Co(II) sorption at low pH, but suppressed Co(II) sorption at high pH. The thermodynamic data derived from temperature dependent sorption isotherms suggested that the sorption of Co(II) on Bi–Mt was spontaneous and endothermic process. Outer-sphere surface complexation and/or ion exchange were the main mechanisms of Co(II) sorption on Bi–Mt at low pH, whereas inner-sphere surface complexation was the main sorption mechanism at high pH. From the experimental results, it is possible to conclude that Bi–Mt is suitable for application of Co(II) removal from aqueous solutions.

1. Introduction

Water pollution by radionuclides through the discharge of industrial waste is a worldwide environmental problem. The presence of radionuclides and their fission products, even at low concentrations, is of major concern, as they pose serious chemical and radiological toxicity threats to living organisms [1]. Radionuclide ^{60}Co is one of the most problematic waste nuclides, due to its relatively long half-life (5.2 a) and high gamma decay energy which is widely used in research and medical applications. Its high doses cause paralysis, diarrhea, low blood pressure, lung irritations and bone defects [2]. Thereby, the removal of ^{60}Co from wastewater is necessary. At present, the most promising and practical approach for removing ^{60}Co is the addition of non-nutritive adsorptive materials to contaminated water. A variety of natural and synthetic materials such as bentonite [3], MgO, MnO_2, TiO_2, SnO [4], γ-Al_2O_3 [5], Mexican aluminosilicates [6], chitosan derivatives [7] and carboxylate-functionalized polyacrylamide grafted lignocellulosics [8] have been tested as cobalt adsorbents. Of all the materials, clays have attracted much attention owing to its high cation exchange capacity, large surface area and low cost and ready availability [9].

Montmorillonite, one of the most abundant clay minerals at the earth surface, is found to be an effective adsorbent for the removal of radionuclides from wastewater [10]. Montmorillonite is composed of units made up of two silica tetrahedral sheets with a central alumina octahedral sheet [11]. The tetrahedral and octahedral sheets combine in such a way that the tips of the tetrahedra of each silica sheet and one of the hydroxyl layers of the octahedral sheet form a common layer. The atoms in this layer, which are common to both sheets, become oxygen instead of hydroxyl. It is thus referred to as a three-layered clay mineral with T–O–T layers making up the structural unit. The replacement of Al^{3+} or occasionally Fe^{3+} for Si^{4+} in the tetrahedral layer, as well as Mg^{2+}, Fe^{2+}, or Mn^{2+} for Al^{3+} in the octahedral layer, give rise to a deficiency of the positive charge in the framework. The charge imbalance is offset by exchangeable cations such as H^+, Na^+, or Ca^{2+} on the layer surfaces. It is possible to modify the surface properties of clays greatly by replacing the cations with inorganic species. This method is inorganic pillaring, using polyhydroxocations such as Al, Zr, Ti, Cr, and Fe [12]. The advantages of pillared montmorillonite include increased surface area and pore volumes, which results in greater sorption capacity and better flow properties as compared to the raw montmorillonite.

Nowadays, a variety of pillared montmorillonites have been used to remove heavy metals from wastewater [13–19]. Cd(II) sorption was increased by the presence of poly-hydroxyl ferric on montmorillonite [13]. Cr(VI) sorption was enhanced by the

* Corresponding author.
E-mail address: xujz@lzu.edu.cn (J. Xu).

0304-3894/$ – see front matter © 2011 Elsevier B.V. All rights reserved.
doi:10.1016/j.jhazmat.2011.05.004

presence of poly-hydroxyl zirconium on montmorillonite [14]. Bouchenafa-Saïb et al. [15] found that the Al pillared montmorillonite has a better affinity towards Cd(II) compared to the raw montmorillonite. However, to the best of our knowledge, the study of Bi pillared montmorillonite, especially its application on the sorption of radiocobalt, is still not available. Our interest in Bi^{3+} modified montmorillonite is due to its remarkably low toxicity, low cost, high versatility and ease of handling [20]. With increasing environmental concerns and the need for 'green reagents', the interest in bismuth and its compounds has increased tremendously in the last decade [21–23].

In this work, Bi pillared montmorillonite (Bi–Mt) was prepared and applied for ^{60}Co(II) removal from aqueous solution to evaluate their feasibilities as novel adsorbent in the environmental remediation. The main purposes of this paper are: (1) to investigate the sorption kinetics of ^{60}Co(II) on Ca-montmorillonite (Ca–Mt) and Bi–Mt and to analyze the experimental data with a pseudo-second-order equation; (2) to study the sorption of ^{60}Co(II) on Bi–Mt as a function of pH, ionic strength, and fulvic acid (FA); (3) to calculate the thermodynamic parameters (i.e., ΔH^0, ΔS^0, ΔG^0) from the temperature dependent sorption isotherms; and (4) to presume the sorption mechanisms of ^{60}Co(II) on Bi–Mt.

2. Materials and methods

2.1. Material

Raw calcium montmorillonite (Ca–Mt) was purchased from Zhejiang Sanding Technology Co. Ltd (Zhejiang, China). The sample contains 98.8% montmorillonite and 1.2% quartz. All chemicals were purchased in analytical purity and used without further purification. Milli-Q water was used in all the experiments. Soil fulvic acid was extracted from the soil of Hua-Jia county (Gansu province, China) and was characterized in detail [24,25]. The main elements are: C 50.15%, H 4.42%, N 5.38%, O 39.56% and S 0.49%.

2.2. Preparation of Bi pillared montmorillonite

Four gram of dry Ca–Mt was added to 200 mL Milli-Q water to get 2% (mass) Ca–Mt suspension, and then the solution was added into 500 mL of $Bi(NO_3)_3{\cdot}5H_2O$ solution (0.006 mol/L, pH 3.5) under vigorous stirring for 2 h at 96 °C. This allows the maximum ion exchange. The suspension was aged for 24 h at room temperature to get bigger crystal particles with better crystallinity. Then the aged suspension was separated by centrifugation, washed several times with Milli-Q water to further purify the residual. The obtained material was then dried at 60 °C, and pulverized to pass through a 200-mesh sieve.

2.3. Characterization

The XRD patterns of Ca–Mt and Bi–Mt were obtained using a D/Max-rB equipped with a rotation anode using Cu Kα radiation (λ = 0.15406 nm). The XRD device was operated at 40 kV and 80 mA. The surface structural groups of Ca–Mt and Bi–Mt were characterized by Fourier Transforms Infrared spectra (FT-IR). The sample for the FT-IR measurement was mounted on a Bruker EQUINOX55 spectrometer (Nexus) in KBr pellet at room temperature. BET surface area measurement was carried out using BEL SORP MINI II, Japan. The samples were degassed at 323 K for 16 h in vacuum prior to analysis. The nitrogen adsorption was carried out at 77 K. The cation exchange capacity (CEC) was measured using the ammonium acetate method through potentiometric titration. The amount of loaded Bi was measured using ICP-OES (Optima 5300DV Spectrometer).

2.4. Experimental procedure

The sorption of Co(II) on Bi–Mt was investigated by using batch technique in polyethylene centrifuge tubes under ambient conditions. The stock suspension of Bi–Mt and $NaClO_4$ solution were first contacted for 24 h to achieve the equilibration of Bi–Mt and $NaClO_4$. Then, cobalt stock solution and FA stock solution were added to achieve the desired concentrations of different components. The system was adjusted to the desired pH by adding negligible volumes of 0.01 or 0.1 mol/L $HClO_4$ or NaOH. After the suspensions were shaken for 48 h, the solid and liquid phases were separated by centrifugation at 7788 g for 30 min.

Radiotracer ^{60}Co(II) was used in the experiments. The concentration of ^{60}Co(II) was analyzed by liquid scintillation counting using a Packard 3100 TR/AB Liquid Scintillation Analyzer (PerkinElmer). The scintillation cocktail was ULTIMA GOLD AB™ (Packard). The amount of Co(II) adsorbed on Bi–Mt was calculated from the difference between the initial concentration and the equilibrium one. All the experimental data were the averages of triplicate determinations and the average uncertainties were about 5%.

The sorption of Co(II) was expressed in terms of distribution coefficient (K_d) and sorption percentage (%), which were derived from the following equations:

$$K_d = \frac{C_0 - C_e}{C_e}\frac{V}{m} \quad (1)$$

$$\text{Sorption}(\%) = \frac{C_0 - C_e}{C_0} \times 100\% \quad (2)$$

where C_0 is the initial concentration, C_e is the equilibrium concentration in supernatant after centrifugation, m is the mass of Bi–Mt, and V is the volume of the suspension. To take into consideration of Co(II) loss from procedures expect for montmorillonite sorption (i.e., Co(II) sorption on centrifuge tube wall), calibration curves were attained separately under otherwise identical conditions as the sorption process but no montmorillonite. Based on the attained calibration curves, we can conclude that the sorption of Co(II) on the centrifuge tube wall was negligible.

3. Results and discussion

3.1. Characterization

3.1.1. X-ray diffraction of montmorillonites

Basal spacing is one of the most important factors reflecting the structural characterization of modified montmorillonite. Fig. 1A presents the XRD patterns of Ca–Mt and Bi–Mt. The d_{001} reflection for basal spacing determined by XRD is found to shift from 1.52 nm (original Ca–Mt) to 1.58 nm in Bi–Mt. This change reveals that Bi has been intercalated into the interlayer space of Ca–Mt.

3.1.2. FT-IR spectra of montmorillonites

Fig. 1B shows the infrared spectra of Ca–Mt and Bi–Mt. The spectral regions of interest are the H–O–H bending region and –OH stretching region of H_2O. The H–O–H bending region (1600–1700 cm^{-1}) and the O–H stretching region (3100–3700 cm^{-1}) are attributed to the physical adsorbed water.

FT-IR spectrum of the Ca–Mt shows the characteristic bands in the –OH stretching region, which may correspond to Al–O–H group (3623 cm^{-1}) and H–O–H group (3422 cm^{-1}). Bending vibrations of water molecules may contribute to –OH peaks (1642 cm^{-1}). The band at about 1034 cm^{-1} in the stretching mode region is due to Si–O–Si, and bands centered at ~469 and 520 cm^{-1} in the stretching mode are due to Si–O–Al and Si–O–Mg, respectively. After the modification of Bi to Ca–Mt, the band at 3422 cm^{-1} (Ca–Mt) shifts

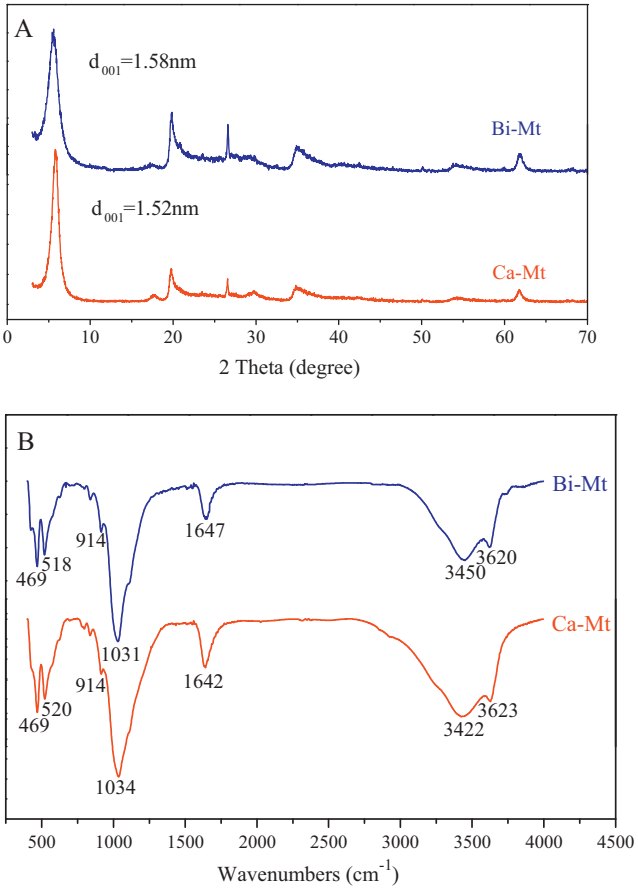

Fig. 1. XRD patterns (A) and FT-IR spectra (B) of montmorillonite samples.

to 3450 cm^{-1} (Bi–Mt) and the band intensity also drops due to the replacement of hydrated inorganic cations of the clay mineral with intercalated bismuth ions during the exchange reaction.

3.1.3. Basic physicochemical properties of montmorillonites

The cation exchange capacity (CEC), the specific surface area, total pore volume, average pore diameter and the amount of loaded Bi are shown in Table 1.

3.2. Results of the sorption experiments

3.2.1. Effect of contact time and kinetics study

The effects of contact time on the removal of Co(II) by Ca–Mt and Bi–Mt are shown in Fig. 2. Both the sorption processes are rapid during the first 30 min contact time and then achieve equilibrium within 2 h. The fast sorption process at the initial stage can be attributed to the fact that the cobalt ions can interact easily with the sites, and the slow sorption rate in later stage is due to slower diffusion of solute into the interior of the adsorbent. Maximum sorption occurs after 2 h and there is almost no further sorption beyond this time. Thus, the shaking time was fixed to 24 h to make sure the sorption can achieve complete equilibrium. This characteristic is desirable for the treatment of industrial wastewater and for emergency use.

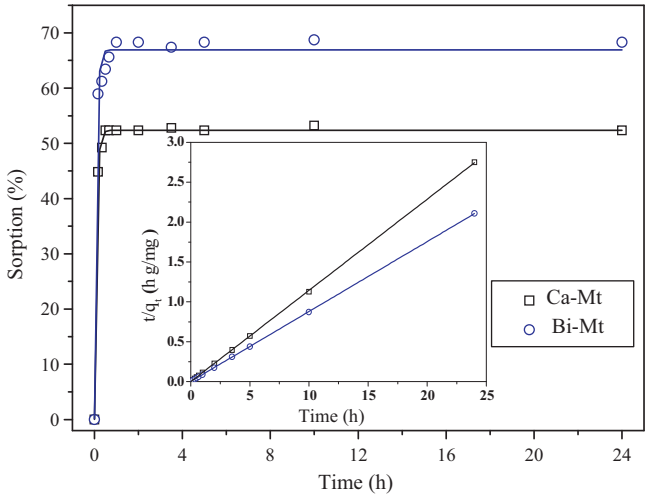

Fig. 2. Effect of contact time on Co(II) sorption on Bi–Mt and Ca–Mt and the pseudo-second-order rate equation fit (insert). Ph 6.0 ± 0.1, I = 0.01 mol/L $NaClO_4$, T = 303.15 K, m/V = 0.6 g/L, $C_{Co(II)initial}$ = 1.67 × 10^{-4} mol/L.

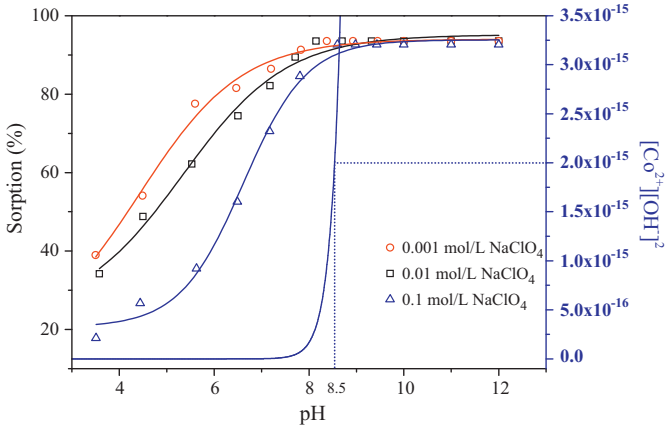

Fig. 3. Effect of ionic strength on Co(II) sorption on Bi–Mt as a function of pH. T = 303.15 K, m/V = 0.6 g/L, $C_{Co(II)initial}$ = 1.67 × 10^{-4} mol/L.

In order to determine the mechanism of the sorption process, the pseudo-second-order model is used to analyze the experimental data. The linear form of this model can be expressed as:

$$\frac{t}{q_t} = \frac{1}{2Kq_e^2} + \frac{1}{q_e}t \quad (3)$$

where q_t (mg/g) is the amount of Co(II) adsorbed at time t, q_e (mg/g) is the equilibrium sorption capacity and K (g/(mg h)) is the pseudo-second-order rate constant. The correlation coefficient (R^2 = 0.999) of the linear plot of t/q_t versus t (the inserted figure in Fig. 2) is very close to 1, which suggests that the experimental data can be fitted very well by the pseudo-second-order model [26–28].

3.2.2. Effect of initial solution pH

Initial pH of the aqueous solution is an important variable that influences the sorption of metal ions at water–solid interfaces. Fig. 3 shows the sorption of Co(II) on Bi–Mt at various pH values ranging

Table 1
Basic physicochemical properties of Ca–Mt and Bi–Mt.

Samples	CEC (cmol/kg)	BET surface area (m^2/g)	Total pore volume (mL/g)	Average pore diameter (Å)	Amount of loaded Bi (mol/kgMt)
Ca–Mt	95.2	26.33	0.0633	101.43	–
Bi–Mt	86.1	75.21	0.0994	58.44	0.18

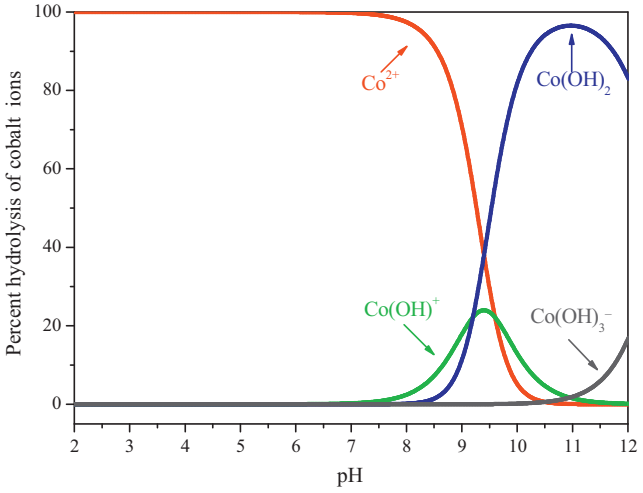

Fig. 4. Relative proportion of Co(II) species as a function of pH. I = 0.01 mol/L $NaClO_4$, T = 303.15 K, $C_{Co(II)} = 1.67 \times 10^{-4}$ mol/L.

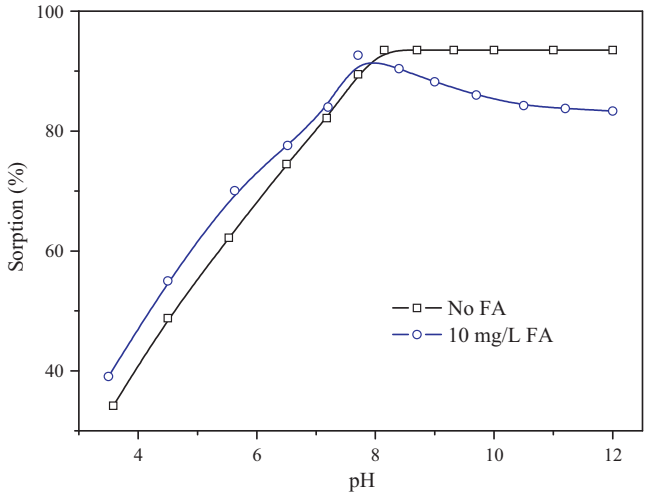

Fig. 5. Effect of FA on Co(II) sorption on Bi–Mt as a function of pH. T = 303.15 K, m/V = 0.6 g/L, C_{FA} = 10 mg/L, $C_{Co(II)initial} = 1.67 \times 10^{-4}$ mol/L.

from 3 to 12 at T = 303.15 K. It is evident that the removal of Co(II) by Bi–Mt is highly pH-dependent. The sorption percentage increases gradually from ~20% to ~93% at pH 3–8.5, and then maintains the high level with increasing pH. In aqueous systems, the surface groups of Bi–Mt can be protonated in different extents. Therefore, the concentrations of surface sites of Bi–Mt change under different pH values. With increasing pH, the surface sites are deprotonated and the hydrolysis of Co(II) also increases. According to the hydrolysis constants of Co(II) ($\log K_1 = -9.6$, $\log K_2 = -9.2$, and $\log K_3 = -12.7$) [29], the distribution species of Co(II) as a function of pH is shown in Fig. 4. The results demonstrate that Co(II) presents in the forms of Co^{2+}, $Co(OH)^+$, $Co(OH)_2$ and $Co(OH)_3^-$ at various pH values. At pH < 8.5, the main species is Co^{2+} and the removal of Co^{2+} is mainly accomplished via sorption reaction. The sorption of Co^{2+} can be attributed to ion exchange between Co^{2+} and H^+/Ca^{2+} on the surface sites. At pH 8.5–12, the predominant species are $Co(OH)^+$ and $Co(OH)_2$ and they are easily to be adsorbed on the negatively charged Bi–Mt surfaces. As a result, the removal of Co(II) maintains a high level and reaches maximum [30]. The precipitation constant of $Co(OH)_2(s)$ is 2×10^{-15}, and the precipitation curve of Co(II) at the concentration of 1.67×10^{-4} mol/L is also shown in Fig. 3. From the precipitation curve, one can see that Co(II) begins to form precipitation at pH ~8.5 if no Co(II) is adsorbed on Bi–Mt. However, ~90% Co(II) is adsorbed on Bi–Mt at pH~8, the precipitation of $Co(OH)_2$ on Co(II) sorption can be negligible because large amounts of Co(II) are adsorbed on Bi–Mt.

3.2.3. Effect of ionic strength

The effect of ionic strength on the removal of Co(II) to Bi–Mt is carried out in 0.001, 0.01 and 0.1 M $NaClO_4$ solutions (Fig. 3). It is clear that the sorption of Co(II) on Bi–Mt at pH < 8.5 is influenced by ionic strength obviously, whereas no drastic difference of Co(II) sorption is found at pH > 8.5 in the three different $NaClO_4$ concentrations. The ionic strength can influence the double layer thickness and interface potential, thereby can affect the binding of the adsorbed species. Ion exchange or outer-sphere surface complexation is influenced by ionic strength obviously, and inner-sphere surface complexation is not affected by ionic strength [31,32]. From the above results, one can conclude that sorption of Co(II) on Bi–Mt is dominated by ion exchange and/or outer-sphere surface complexation at low pH, and by inner-sphere surface complexation at high pH [33].

3.2.4. Effect of FA

Fig. 5 illustrates the pH-dependent of Co(II) sorption on Bi–Mt in the absence and presence of FA. As can be seen from Fig. 5, a positive effect of FA on the sorption of Co(II) on Bi–Mt is observed at pH < 8, while a negative effect of FA is observed at pH > 8. At low pH values, the negatively charged FA can be easily adsorbed on the positively charged Bi–Mt surface. The strong complexation ability of Co(II) ions with surface adsorbed FA results in the increasing sorption of Co(II) on Bi–Mt [34]. However, at high pH values, the negatively charged FA is difficult to be adsorbed on the negatively charged Bi–Mt surface due to electrostatic repulsion. The fraction of FA remained in solution increases with increasing pH values, and soluble FA-Co(II) complexes are formed in solution and thereby reduces Co(II) sorption at high pH values [35]. However, the effect of FA on metal ion sorption is very complicated and various results have been reported. Zhao et al. [36] found that the presence of FA enhanced the sorption of Pb(II) on β-MnO_2 at pH < 7, while reduced Pb(II) sorption at pH > 7. Tan et al. [37] concluded that the presence of FA increased Eu(III) sorption on TiO_2 at pH < 6, while the presence of FA had no influence on the sorption at higher pH values. Fan et al. [38] investigated Ni(II) sorption on Na-attapulgite and found that the presence of FA had no influence on the sorption of Ni(II) at low pH, while decreased the sorption of Ni(II) at high pH values. The differences reported in the above-mentioned literatures are attributed to many factors such as the nature of humic substances, nature of minerals, nature of metal ions, solution pH and, etc.

3.2.5. Effect of Bi–Mt content

The sorption of Co(II) on Bi–Mt as a function of solid content is shown in Fig. 6. The removal of Co(II) from solution to Bi–Mt increases with increasing Bi–Mt content. With increasing solid content, the functional groups at the Bi–Mt surfaces increase and thereby more surface sites are available to form complexes with Co(II) at solid surfaces. The distribution coefficient (K_d) values of Co(II) sorption on Bi–Mt are also shown in Fig. 6. The K_d values are constant with increasing solid contents, which are consistent with the physicochemical properties of K_d values, i.e., the K_d value is independent of solid content at low solid content [39]. The results suggest that there is almost no competition among the functional groups at Bi–Mt surfaces. Because of the low content of Bi–Mt in the system, the particles of Bi–Mt are almost not aggregated in the suspension. The Co(II) ions in solution can freely form complexes at the surfaces of Bi–Mt, and this reaction is not affected by the content of Bi–Mt [40].

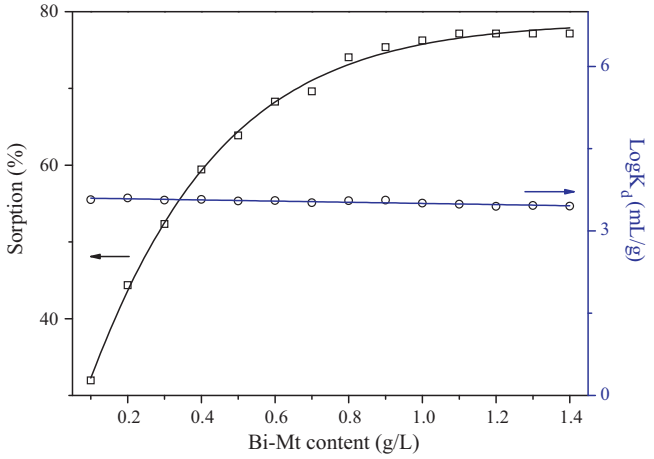

Fig. 6. Effect of solid content on Co(II) sorption on Bi–Mt. pH 6.0 ± 0.1, I = 0.01 mol/L $NaClO_4$, T = 303.15 K, $C_{Co(II)initial}$ = 1.67 × 10^{-4} mol/L.

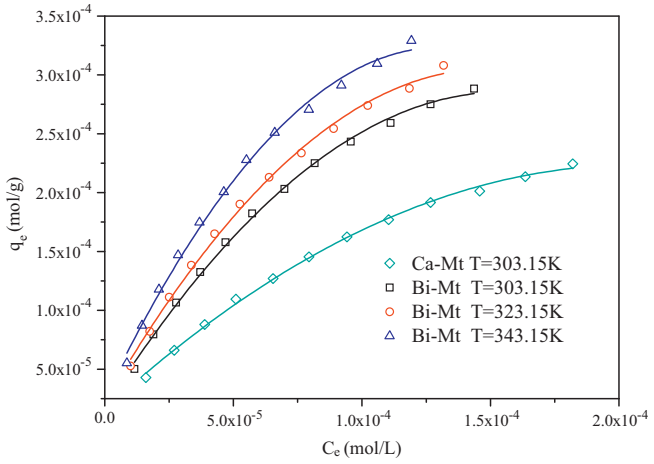

Fig. 7. Sorption isotherms of Co(II) on Bi–Mt and Ca–Mt at different temperatures. I = 0.01 mol/L $NaClO_4$, pH 6.0 ± 0.1, m/V = 0.6 g/L.

3.2.6. Sorption isotherms of Co(II) on Ca–Mt and Bi–Mt

The sorption of Co(II) on Ca–Mt at 303.15 K and on Bi–Mt at 303.15, 323.15 and 343.15 K, respectively, are shown in Fig. 7. One can see that the sorption isotherm of Co(II) on Bi–Mt is much higher than that on Ca–Mt at 303.15 K, indicating that Bi–Mt has higher affinity towards Co(II) than Ca–Mt. The sorption isotherm of Co(II) on Bi–Mt is the highest at T = 343.15 K and is the lowest at T = 303.15 K, indicating that high temperature is advantageous for Co(II) sorption on Bi–Mt. Langmuir, Freundlich and D–R isotherm models are conducted to simulate the sorption data of Co(II) on Ca–Mt and Bi–Mt.

The Langmuir isotherm is valid for monolayer sorption onto a surface with a finite number of identical sites. This model is based on the assumption of sorption homogeneity, such as equally available sorption sites, monolayer surface coverage, and no interaction between adsorbed species. Its form can be expressed as [41]:

$$\frac{C_e}{q_e} = \frac{1}{bq_{max}} + \frac{C_e}{q_{max}} \quad (4)$$

where C_e (mg/L) is the equilibrium concentration of Co(II) in solution, q_e (mol/g) is the amount of Co(II) adsorbed on per weight unit of solid after equilibrium, q_{max} (mol/g) is the maximum sorption capacity and b (L/mol) is a constant that relates to the heat of sorption.

The Freundlich model is an empirical equation with the assumption that the sorption energy of Co(II) binding to a site on an adsorbent depends on whether or not the adjacent sites are already occupied. This model is usually appropriate for heterogeneous sorption with the form as follows [42]:

$$\log q_e = \log k_F + n \log C_e \quad (5)$$

where k_F (mol^{1-n} L^n/g) is the Freundlich constant which is related to sorption capacity. n is a constant representing the mutual interaction of adsorbed species. Experimental values of n are usually greater than unity and this means that the forces between the adsorbed molecules are repulsive.

The D–R isotherm, apart from being an analogue of the Langmuir isotherm, is more general than the Langmuir model, since it does not assume a homogeneous surface or constant sorption potential [43]. This model can be used to estimate the characteristic porosity of adsorbents and their apparent energy of sorption. Its form can be described as follows:

$$\ln q_e = \ln q_{max} - \beta\varepsilon^2 \quad (6)$$

where β is the activity coefficient related to the mean sorption energy (mol^2/kJ^2), and ε is the Polanyi potential, which is equal to:

$$\varepsilon = RT \ln\left(1 + \frac{1}{Ce}\right) \quad (7)$$

where R is ideal gas constant (8.314 J/(mol K)), and T is the absolute temperature in Kelvin (K).

The experimental data of Co(II) sorption are analyzed with the Langmuir, Freundlich and D–R models, and the results are shown in Fig. 8. The relative parameters are listed in Table 2. It can be concluded from the correlation coefficients that Langmuir model simulates the experimental data better than Freundlich and D–R models. The fact that the sorption data of Co(II) according with Langmuir isotherm suggests that the binding energy on the whole surface of Bi–Mt is uniform. In other words, the whole surface has identical sorption activity and therefore the adsorbed Co(II) ions do not interact or compete with each other, and they are adsorbed by forming an almost complete monolayer coverage of the Bi–Mt particles. This phenomenon also suggests that chemisorption is the principal uptake mechanism in sorption process. Moreover, Bi–Mt has a finite surface area and sorption capacity, thus the sorption could be better described by Langmuir model rather than by Freundlich model, as an exponentially increasing sorption was assumed in the Freundlich model. At all temperatures, the value of q_e was found to be smaller than q_{max}, which suggests that Co(II) sorption on Bi–Mt is by a monolayer type in which the surface of

Table 2
The parameters for Langmuir, Freundlich and D–R sorption isotherms of Co(II) on Ca–Mt and Bi–Mt.

Adsorbent	T (K)	Langmuir			Freundlich			D–R		
		q_{max} (mol/g)	b (L/mol)	R^2	K_F (mol^{1-n} L^n/g)	n	R^2	β (mol^2/kJ^2)	q_{max} (mol/g)	R^2
Ca–Mt	303.155	3.82×10^{-4}	7.80×10^{3}	0.999	8.03×10^{-2}	0.674	0.989	5.27×10^{-3}	4.70×10^{-3}	0.995
Bi–Mt	303.15	4.92×10^{-4}	1.01×10^{4}	0.999	1.37×10^{-1}	0.685	0.985	5.10×10^{-3}	4.91×10^{-3}	0.993
Bi–Mt	323.15	5.14×10^{-4}	1.11×10^{4}	0.999	1.43×10^{-1}	0.679	0.988	4.79×10^{-3}	3.08×10^{-3}	0.995
Bi–Mt	343.15	5.27×10^{-4}	1.36×10^{4}	0.999	1.45×10^{-1}	0.665	0.985	4.19×10^{-3}	4.51×10^{-3}	0.993

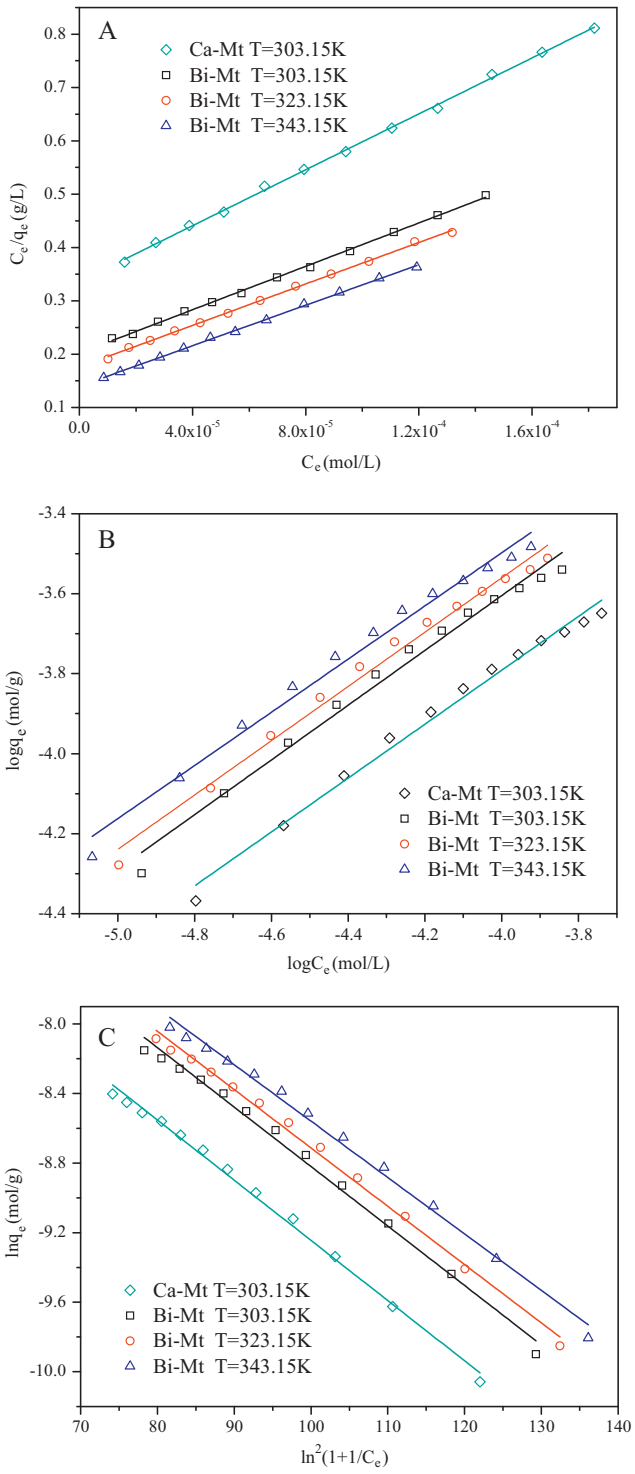

Fig. 8. Langmuir (A), Freundlich (B) and D–R (C) model fittings for Co(II) sorption on Bi–Mt at three different temperatures. I = 0.01 mol/L $NaClO_4$, pH 6.0 ± 0.1, m/V = 0.6 g/L.

Bi–Mt is not saturated. The value of n calculated from the Freundlich model is from unity, indicating that a nonlinear sorption of Co(II) takes place on Bi–Mt surfaces.

3.2.7. Thermodynamic study

The thermodynamic parameters (ΔH^0, ΔS^0 and ΔG^0) for Co(II) sorption on Bi–Mt are calculated from the temperature dependent sorption isotherms. The Gibbs free energy change (ΔG^0) is calculated from the following equation:

$$\Delta G^0 = -RT \ln K^0 \quad (8)$$

where R is ideal gas constant (8.314 J/(mol K)), K^0 is the sorption equilibrium constant. The values of $\ln K^0$ are obtained by plotting $\ln K_d$ versus C_e (Fig. 9) and extrapolating C_e to zero [44]. Standard entropy change (ΔS^0) is calculated using the equation:

$$\Delta S^0 = -\left(\frac{\partial \Delta G^0}{\partial T}\right)_P \quad (9)$$

The average standard enthalpy change (ΔH^0) is then calculated from the expression:

$$\Delta H^0 = \Delta G^0 + T\Delta S^0 \quad (10)$$

The values obtained from Eqs. (8)–(10) are tabulated in Table 3. The positive value of the standard enthalpy change indicates that the sorption is endothermic, which suggests the existence of a strong interaction between Bi–Mt with Co(II). One possible explanation to this positive entropy is that Co(II) is solved well in water, and the hydration sheath of Co(II) has to be destroyed before its sorption on Bi–Mt. This dehydration process needs energy, and it is favored at high temperature [36,45]. The implicit assumption is that after sorption the environment of Co(II) ions is less aqueous than it is in solution. The removal of water from ions is substantially an endothermic process, and it appears that the endothermicity of the desolvation process exceeds that of the enthalpy of sorption by a considerable extent. The Gibbs free energy change (ΔG^0) is negative as expected for a spontaneous process under the conditions applied. The value of ΔG^0 becomes more negative with the increase of temperature, indicating more efficient sorption at high temperature. At high temperature, cations are readily desolvated and hence their sorption becomes more favorable [46]. The positive value of entropy change (ΔS^0) implies some structural changes in adsorbate and adsorbent during the sorption process, which leads to an increase in the disorder of the solid-solution

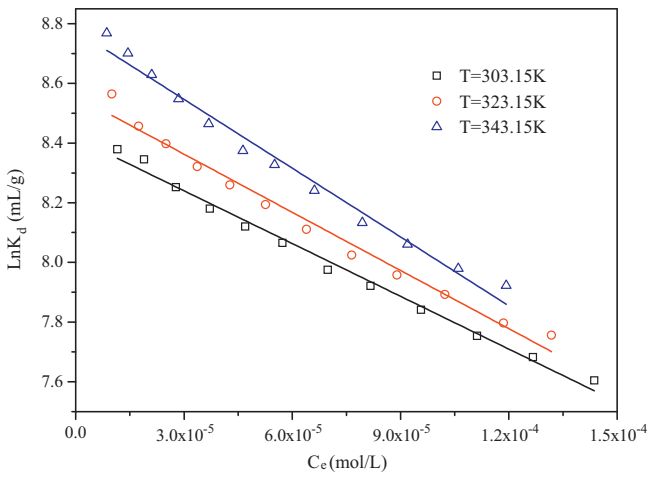

Fig. 9. Linear plots of $\ln K_d$ versus C_e for Co(II) sorption on Bi–Mt at three different temperatures. I = 0.01 mol/L $NaClO_4$, pH 6.0 ± 0.1, m/V = 0.6 g/L.

Table 3
Values of thermodynamic parameters for the sorption of Co(II) on Bi–Mt.

T (K)	ΔG^0 (kJ/mol)	ΔH^0 (kJ/mol)	ΔS^0 (J/(mol/K))
303.15	−21.21	7.77	95.6
323.15	−22.99	7.90	95.6
343.15	−25.04	7.77	95.6

Table 4
Comparison of Co(II) sorption capacities of Bi–Mt with other adsorbents.

Adsorbent	Sorption capacity (mg/g)	Solution chemistry conditions	Reference
Granular activated carbon	1.19	pH 6.0 T = 298.15 K	[47]
Polymeric chitosan adsorbent	5.11	pH 8.0 T = 298.15 K	[7]
ZrO–kaolinite	9.60	pH 5.8 T = 303.15 K	[19]
Coir pith	12.82	pH 4.3 T = 300.15 K	[48]
Natural zeolite	14.65	pH 6–7 T = 303.15 K	[49]
Bentonite	16.92	pH 7.0 T = 298.15 K	[3]
Hydroxyapatite	20.92	pH 5.0 T = 293.15 K	[50]
Formaldehyde Modified-bentonite	21.78	pH 7.0 T = 298.15 K	[3]
Lemon peel	22.00	pH 6.0 T = 298.15 K	[51]
ZrO-montmorillonite	22.80	pH 5.8 T = 303.15 K	[19]
Bi–Mt	29.52	pH 6.0 T = 303.15 K	This work
PGBS–COOH	166.70	pH 6.5 T = 303.15 K	[8]

system. The thermodynamic analysis derived from temperature dependent sorption isotherms suggests that the sorption process of Co(II) on Bi–Mt is spontaneous and endothermic [38].

3.2.8. Comparison of sorption capacity of Bi–Mt with other adsorbents

The maximum sorption capacity of Bi–Mt is compared with other materials (see Table 4). Although a direct comparison of Bi–Mt with other adsorbents is difficult due to the different experimental conditions applied, it has been found that Co(II) sorption capacity of Bi–Mt is higher than that of granular activated carbon, polymeric chitosan adsorbent, ZrO–kaolinite, coir pith, natural zeolite, bentonite, hydroxyapatite, formaldehyde modified-bentonite, lemon peel and ZrO-montmorillonite. The low cost and simplicity of preparation process make Bi–Mt an attractive adsorbent for the cost-effective treatment of Co-bearing wastewater.

4. Conclusions

In this study, the sorption of Co(II) on raw Ca–Mt and Bi–Mt was investigated by using batch technique. Compared to raw Ca–Mt, Bi–Mt showed a higher affinity to bind Co(II) ions. In addition, the sorption percentage of Co(II) on Bi–Mt increased with increasing pH at pH 3–8.5, and then maintained the high level at pH 8.5–12. The sorption of Co(II) on Bi–Mt was dependent on ionic strength at low pH values, and independent of ionic strength at high pH values. The presence of FA enhanced Co(II) sorption on Bi–Mt at low pH values, but suppressed Co(II) sorption at high pH values. The thermodynamic analysis derived from temperature dependent sorption isotherms suggested that the sorption of Co(II) on Bi–Mt is an spontaneous and endothermic process. By integrating all the above-mentioned analysis results together, one can conclude that outer-sphere surface complexation and/or ion exchange are the main mechanisms of Co(II) sorption on Bi–Mt at low pH values, whereas inner-sphere surface complexation is the main sorption mechanism at high pH values. Considering its high affinity to bind Co(II) ions and the simplicity of preparation process, one can conclude that Bi–Mt is suitable for potential practical application in heavy metal ion pollution disposal.

Acknowledgement

Financial support from the 973 project (2008CB417212) is acknowledged.

References

[1] J.E. Till, H.A. Grogan, Radiological Risk Assessment and Environmental Analysis, Oxford University press, New York, 2008.
[2] V.P. Kudesia, Water Pollution, Pregatiprakashan Publications, Meerut, 1990.
[3] H. Omar, H. Arida, A. Daifullah, Adsorption of ^{60}Co radionuclides from aqueous solution by raw and modified bentonite, Appl. Clay Sci. 44 (2009) 21–26.
[4] F. Granados, V. Bertin, S. Bulbulian, M. Solache-Rios, ^{60}Co aqueous speciation and pH effect on the adsorption behavior on inorganic materials, Appl. Radiat. Isot. 64 (2006) 291–297.
[5] E.J. Boyle-Wight, L.E. Katz, K.F. Hayes, Macroscopic studies of the effects of selenate and selenite on cobalt sorption to γ-Al_2O_3, Environ. Sci. Technol. 36 (2002) 1212–1218.
[6] J.I. Davila-Rangel, M. Solache-Rios, J.E. Nunez-Monreal, Radiation and thermal effects on cobalt retention by Mexican aluminosilicates, J. Nucl. Mater. 362 (2007) 53–59.
[7] E. Metwally, S.S. Elkholy, H.A.M. Salem, M.Z. Elsabee, Sorption behavior of ^{60}Co and $^{152+154}$Eu radionuclides onto chitosan derivatives, Carbohydr. Polym. 76 (2009) 622–631.
[8] I.G. Shibi, T.S. Anirudhan, Adsorption of Co(II) by a carboxylate-functionalized polyacrylamide grafted lignocellulosics, Chemosphere 58 (2005) 1117–1126.
[9] H.H. Murray, Traditional and new applications for kaolin, smectite, and palygorskite: a general overview, Appl. Clay Sci. 17 (2000) 207–221.
[10] J.J. Wu, B. Li, J.L. Liao, Y. Feng, D. Zhang, J. Zhao, W. Wen, Y.Y. Yang, N. Liu, Behavior and analysis of cesium adsorption on montmorillonite mineral, J. Environ. Radioact. 100 (2009) 914–920.
[11] C.E. Marshall, Layer lattice and base-exchange of clays, Z Kristallogr. 91 (1935) 433–449.
[12] R.T. Yang, M.S.A. Baksh, Pillared clays as a new class of sorbents for gas separation, AIChE J. 37 (1991) 679–686.
[13] P.X. Wu, W.M. Wu, S.Z. Li, N. Xing, N.W. Zhu, P. Li, J.H. Wu, C. Yang, Z. Dang, Removal of Cd^{2+} from aqueous solution by adsorption using Fe-montmorillonite, J. Hazard. Mater. 169 (2009) 824–830.
[14] J.B. Zhou, P.X. Wu, Z. Dang, N.W. Zhu, P. Li, J.H. Wu, X.D. Wang, Polymeric Fe/Zr pillared montmorillonite for the removal of Cr(VI) from aqueous solutions, Chem. Eng. J. 162 (2010) 1035–1044.
[15] N. Bouchenafa-Saïb, K. Khouli, O. Mohammedi, Preparation and characterization of pillared montmorillonite: application in adsorption of cadmium, Desalination 217 (2007) 282–290.
[16] L.G. Yan, X.Q. Shan, B. Wen, G. Owens, Adsorption of cadmium onto Al_{13}-pillared acid-activated montmorillonite, J. Hazard. Mater. 156 (2008) 499–508.
[17] A. Ramesh, H. Hasegawa, T. Maki, K. Ueda, Adsorption of inorganic and organic arsenic from aqueous solutions by polymeric Al/Fe modified montmorillonite, Sep. Purif. Technol. 56 (2007) 90–100.
[18] K.G. Bhattacharyya, S.S. Gupta, Kaolinite, montmorillonite, and their modified derivatives as adsorbents for removal of Cu(II) from aqueous solution, Sep. Purif. Technol. 50 (2006) 388–397.
[19] K.G. Bhattacharyya, S.S. Gupta, Adsorption of Fe(III), Co(II) and Ni(II) on ZrO–kaolinite and ZrO-montmorillonite surfaces in aqueous medium, Colloid Surf. A 317 (2008) 71–79.
[20] A.D. Bailey, A.R. Baru, K.K. Tasche, R.S. Mohan, Environmentally friendly organic synthesis using bismuth compounds: bismuth(III) iodide catalyzed deprotection of acetals in water, Tetrahedron Lett. 49 (2008) 691–694.
[21] J.A. Marshall, Organic chemistry of Bi(III) compounds, Chemtracts 10 (1997) 1064–1075.
[22] M. Postel, E. Dunach, Bismuth derivatives for the oxidation of organic-compounds, Coord. Chem. Rev. 155 (1996) 127–144.
[23] N.M. Leonard, L.C. Wieland, R.S. Mohan, Applications of bismuth(III) compounds in organic synthesis, Tetrahedron 58 (2002) 8373–8397.
[24] X.L. Tan, X.K. Wang, H. Geckeis, T.H. Rabung, Sorption of Eu(III) on humic acid or fulvic acid bound to alumina studied by SEM-EDS, XPS, TRLFS and batch techniques, Environ. Sci. Technol. 42 (2008) 6532–6537.
[25] Q.H. Fan, X.L. Tan, J.X. Li, X.K. Wang, W.S. Wu, G. Montavon, Sorption of Eu(III) on attapulgite studied by batch, XPS, and EXAFS techniques, Environ. Sci. Technol. 43 (2009) 5776–5782.
[26] J. Hu, C.L. Chen, X.X. Zhu, X.K. Wang, Removal of chromium from aqueous solution by using oxidized multiwalled carbon nanotubes, J. Hazard. Mater. 162 (2009) 1542–1550.
[27] X.K. Wang, C.L. Chen, J.Z. Du, X.L. Tan, D. Xu, S.M. Yu, Effect of pH and aging time on the kinetic dissociation of ^{243}Am(III) from humic acid-coated γ-Al_2O_3: a chelating resin exchange study, Environ. Sci. Technol. 39 (2005) 7084–7088.
[28] P. Yuan, M.D. Fan, D. Yang, H.P. He, D. Liu, A.H. Yuan, J.X. Zhu, T.H. Chen, Montmorillonite-supported magnetite nanoparticles for the removal of hexavalent chromium[Cr(VI)] from aqueous solutions, J. Hazard. Mater. 166 (2009) 821–829.
[29] H. Yüzer, M. Kara, E. Sabah, M.S. Çelik, Contribution of cobalt ion precipitation to adsorption in ion exchange dominant systems, J. Hazard. Mater. 151 (2008) 33–37.
[30] S.T. Yang, J.X. Li, Y. Lu, Y.X. Chen, X.K. Wang, Sorption of Ni(II) on GMZ bentonite: effects of pH, ionic strength, foreign ions, humic acid and temperature, Appl. Radiat. Isot. 67 (2009) 1600–1608.
[31] B. Baeyens, M.H. Bradbury, A mechanistic description of Ni and Zn sorption on Na-montmorillonite, part I: titration and sorption measurements, J. Contam. Hydrol. 27 (1997) 199–222.

[32] C.L. Chen, X.K. Wang, Sorption of Th (IV) to silica as a function of pH, humic/fulvic acid, ionic strength, electrolyte type, Appl. Radiat. Isot. 65 (2007) 155–163.
[33] S.W. Wang, J. Hu, J.X. Li, Y.H. Dong, Influence of pH, soil humic/fulvic acid, ionic strength, foreign ions and addition sequences on adsorption of Pb(II) onto GMZ bentonite, J. Hazard. Mater. 167 (2009) 44–51.
[34] S.T. Yang, D.L. Zhao, H. Zhang, S.S. Lu, L. Chen, X.J. Yu, Impact of environmental conditions on the sorption behavior of Pb(II) in Na-bentonite suspensions, J. Hazard. Mater. 183 (2010) 632–640.
[35] G.D. Sheng, S.W. Wang, J. Hu, Y. Lu, J.X. Li, Y.H. Dong, X.K. Wang, Adsorption of Pb(II) on diatomite as affected via aqueous solution chemistry and temperature, Colloids Surf. A 339 (2009) 159–166.
[36] D.L. Zhao, X. Yang, H. Zhang, C.L. Chen, X.K. Wang, Effect of environmental conditions on Pb(II) adsorption on β-MnO_2, Chem. Eng. J. 164 (2010) 49–55.
[37] X.L. Tan, M. Fang, J.L. Li, Y. Lu, X.K. Wang, Adsorption of Eu(III) onto TiO_2: effect of pH, concentration, ionic strength and soil fulvic acid, J. Hazard. Mater. 168 (2009) 458–465.
[38] Q.H. Fan, D.D. Shao, Y. Lu, W.S. Wu, X.K. Wang, Effect of pH, ionic strength, temperature and humic substances on the sorption of Ni(II) to Na-attapulgite, Chem. Eng. J. 150 (2009) 188–195.
[39] G.X. Zhao, H.X. Zhang, Q.H. Fan, X.M. Ren, J.X. Li, Y.X. Chen, X.K. Wang, Sorption of copper(II) onto super-adsorbent of bentonite-polyacrylamide composites, J. Hazard. Mater. 173 (2010) 661–668.
[40] J.X. Li, J. Hu, G.D. Sheng, G.X. Zhao, Q. Huang, Effect of pH, ionic strength, foreign ions and temperature on the adsorption of Cu(II) from aqueous solution to GMZ bentonite, Colloids Surf. A 349 (2009) 195–201.
[41] D. Xu, X.L. Tan, C.L. Chen, X.K. Wang, Adsorption of Pb(II) from aqueous solution to MX-80 bentonite: effect of pH, ionic strength, foreign ions and temperature, Appl. Clay Sci. 41 (2008) 37–46.
[42] S.T. Yang, J.X. Li, D.D. Shao, J. Hu, X.K. Wang, Adsorption of Ni(II) on oxidized multi-walled carbon nanotubes: effect of contact time, pH, foreign ions and PAA, J. Hazard. Mater. 166 (2009) 109–116.
[43] G.D. Sheng, D.D. Shao, X.M. Ren, X.Q. Wang, J.X. Li, Y.X. Chen, X.K. Wang, Kinetics and thermodynamics of adsorption of ionizable aromatic compounds from aqueous solutions by as-prepared and oxidized multiwalled carbon nanotubes, J. Hazard. Mater. 178 (2010) 505–516.
[44] G.D. Sheng, J. Hu, X.K. Wang, Sorption properties of Th(IV) on the raw diatomite-effects of contact time, pH, ionic strength and temperature, Appl. Radiat. Isot. 66 (2008) 1313–1320.
[45] G.D. Sheng, J.X. Li, D.D. Shao, J. Hu, C.L. Chen, Y.X. Chen, X.K. Wang, Adsorption of copper(II) on multiwalled carbon nanotubes in the absence and presence of humic or fulvic acids, J. Hazard. Mater. 178 (2010) 333–340.
[46] J. Hu, D.D. Shao, C.L. Chen, G.D. Sheng, X.M. Ren, X.K. Wang, Removal of 1-naphthylamine from aqueous solution by multiwall carbon nanotubes/iron oxides/cyclodextrin composite, J. Hazard. Mater. 185 (2011) 463–471.
[47] A.H. Sulaymon, B.A. Abid, J.A. Al-Najar, Removal of lead copper chromium and cobalt ions onto granular activated carbon in batch and fixed-bed adsorbers, Chem. Eng. J. 155 (2009) 647–653.
[48] H. Parab, S. Joshi, N. Shenoy, A. Lali, U.S. Sarma, M. Sudersanan, Determination of kinetic and equilibrium parameters of the batch adsorption of Co(II), Cr(III) and Ni(II) onto coir pith, Process Biochem. 41 (2006) 609–615.
[49] E. Erdem, N. Karapinar, R. Donat, The removal of heavy metal cations by natural zeolites, J. Colloid Interface Sci. 280 (2004) 309–314.
[50] A. Bhatnagar, A.K. Minocha, M. Sillanpää, Adsorptive removal of cobalt from aqueous solution by utilizing lemon peel as biosorbent, Biochem. Eng. J. 48 (2010) 181–186.
[51] I. Smičiklas, S. Dimović, I. Plećaš, M. Mitrić, Removal of Co^{2+} from aqueous solutions by hydroxyapatite, Water Res. 40 (2006) 2267–2274.